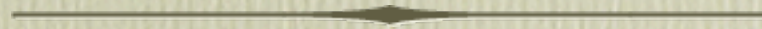


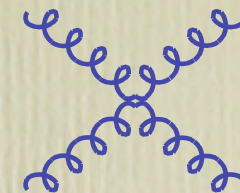
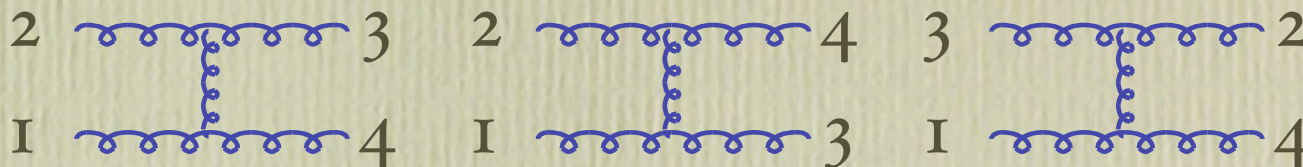
# Introduction to the physics of hard probes in hadron collisions: lecture II



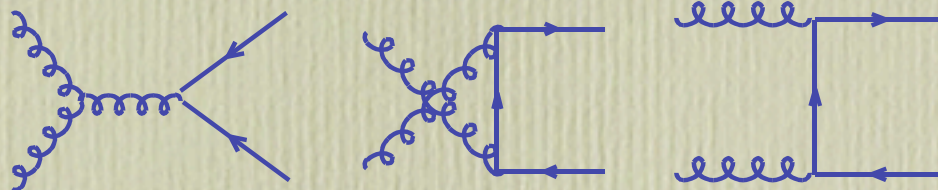
Michelangelo Mangano  
TH Division, CERN  
[michelangelo.mangano@cern.ch](mailto:michelangelo.mangano@cern.ch)

# Jet production

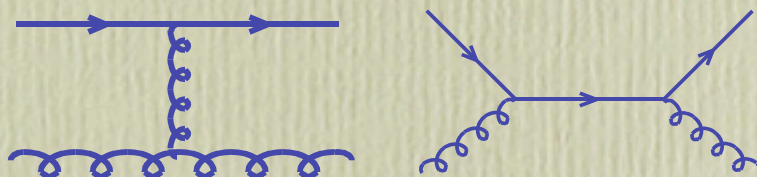
$gg \rightarrow gg$



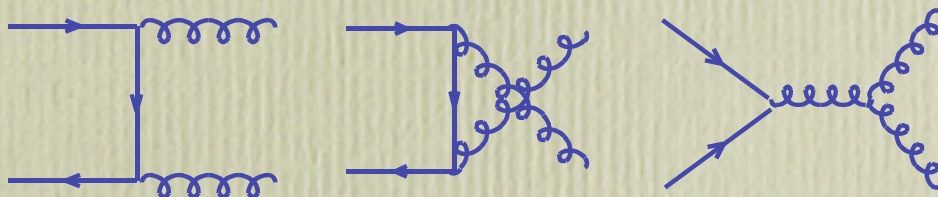
$gg \rightarrow q\bar{q}$



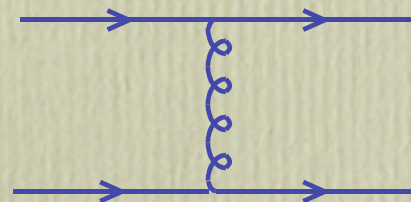
$qg \rightarrow qg$



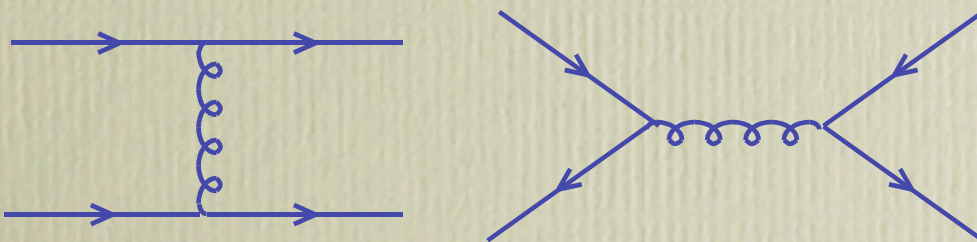
$q\bar{q} \rightarrow gg$



$qq' \rightarrow qq'$



$q\bar{q} \rightarrow q\bar{q}$



- Inclusive production of jets is the largest component of high- $Q$  phenomena in hadronic collisions
- QCD predictions are known up to NLO accuracy
- Intrinsic theoretical uncertainty (at NLO) is approximately 10%
- Uncertainty due to knowledge of parton densities varies from 5-10% (at low transverse momentum,  $p_T$ ) to 100% (at very high  $p_T$ , corresponding to high- $x$  gluons)
- Jets are used as probes of the quark structure (possible substructure implies departures from point-like behaviour of cross-section), or as probes of new particles (peaks in the invariant mass distribution of jet pairs)

# Phase space and cross-section for LO jet production

$$d[PS] = \frac{d^3 p_1}{(2\pi)^2 2p_1^0} \frac{d^3 p_2}{(2\pi)^2 2p_2^0} (2\pi)^4 \delta^4(P_{in} - P_{out}) dx_1 dx_2$$

$$(a) \quad \delta(E_{in} - E_{out}) \delta(P_{in}^z - P_{out}^z) dx_1 dx_2 = \frac{1}{2E_{beam}^2}$$

$$(b) \quad \frac{dp^z}{p^0} = dy \equiv d\eta$$



$$d[PS] = \frac{1}{4\pi S} p_T dp_T d\eta_1 d\eta_2$$



$$\frac{d^3 \eta}{dp_T d\eta_1 d\eta_2} = \frac{p_T}{4\pi S} \sum_{i,j} f_i(x_1) f_j(x_2) \frac{1}{2\hat{s}} \sum_{kl} \overline{|M(ij \rightarrow kl)|^2}$$

The measurement of  $p_T$  and rapidities for a dijet final state uniquely determines the parton momenta  $x_1$  and  $x_2$ . Knowledge of the partonic cross-section allows therefore the determination of partonic densities  $f(x)$

# Some more kinematics

Prove as an exercise that

$$x_{1,2} = \frac{p_T}{E_{beam}} \cosh y^* e^{\pm y_b}$$

where

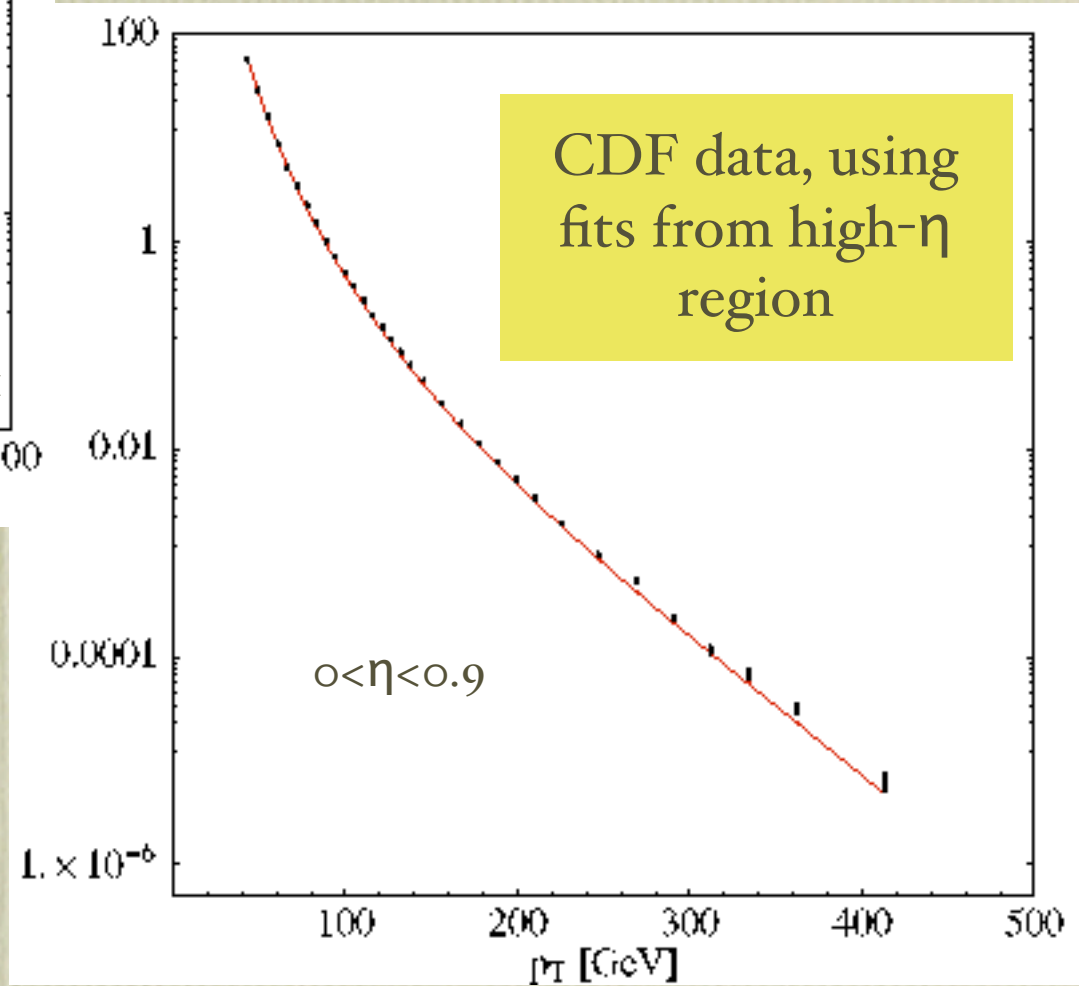
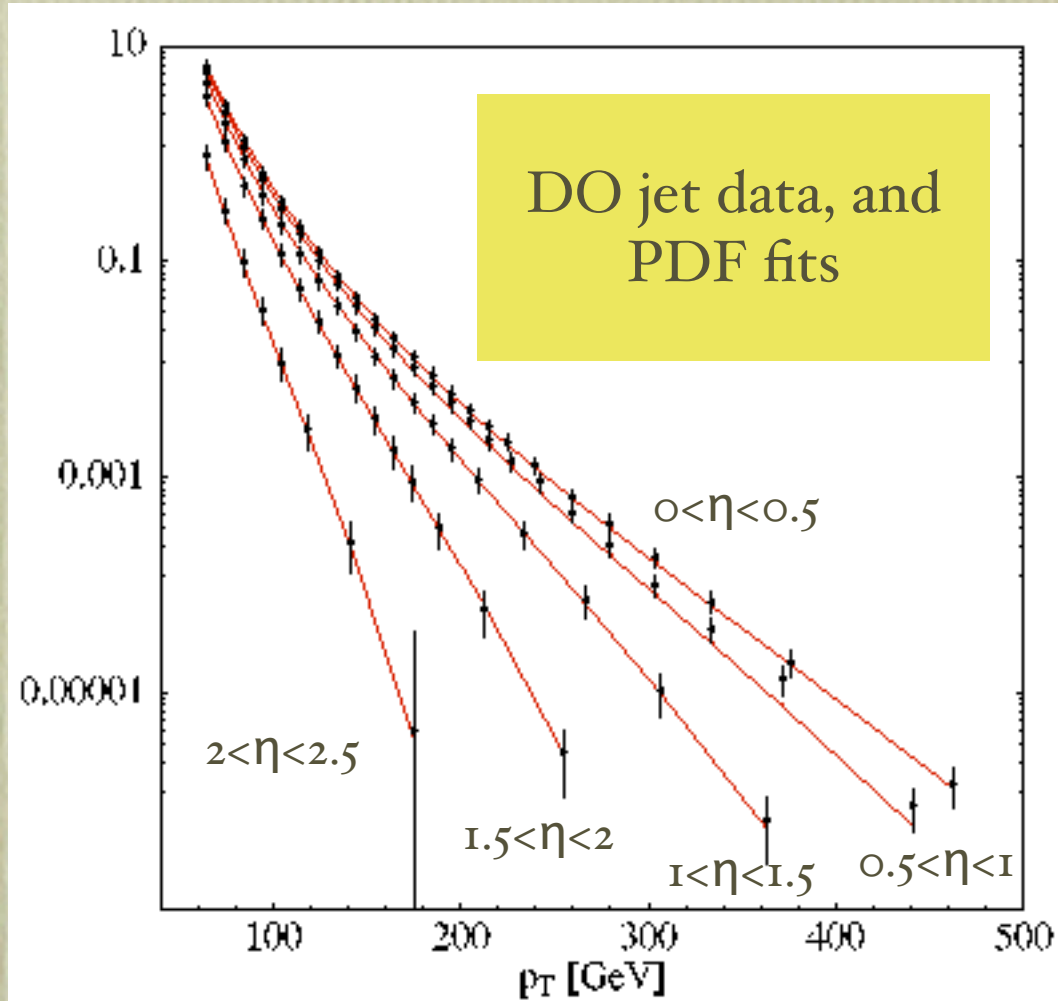
$$y^* = \frac{\eta_1 - \eta_2}{2}, \quad y_b = \frac{\eta_1 + \eta_2}{2}$$

We can therefore reach large values of  $x$  either by selecting large invariant mass events:

$$\frac{p_T}{E_{beam}} \cosh y^* \equiv \sqrt{\bar{\alpha}} \rightarrow 1$$

or by selecting low-mass events, but with large boosts ( $y_b$  large) in either positive or negative directions. In this case, we probe large- $x$  with events where possible new physics is absent, thus setting consistent constraints on the behaviour of the cross-section in the high-mass region, which could hide new phenomena.

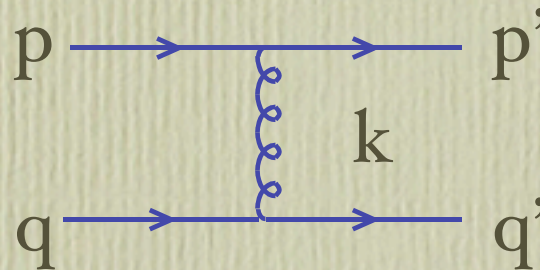
# Example, at the Tevatron



# Small-angle jet production, a useful approximation for the determination of the matrix elements and of the cross-section

At small scattering angle,  $t = (p_1 - p_3)^2 \sim (1 - \cos \theta) \rightarrow 0$

and the  $1/t^2$  propagators associated with t-channel gluon exchange dominate the matrix elements for all processes. In this limit it is easy to evaluate the matrix elements. For example:



$$\sim (\square^a)_{ij} (\square^a)_{kl} (2p_\mu) \frac{1}{t} (2q_\mu) = \frac{2s}{t} (\square^a)_{ij} (\square^a)_{kl}$$

where we used the fact that, for  $k=p-p' \ll p$  (small angle scattering),

$$\bar{u}(p') \square_\mu u(p) \sim \bar{u}(p) \square_\mu u(p) = 2p_\mu$$

Using our colour algebra results, we then get:  $\overline{\square_{col,spin}} |M|^2 = \frac{1}{N_c^2} \frac{N_c^2 - 1}{4} \frac{4s^2}{t^2}$

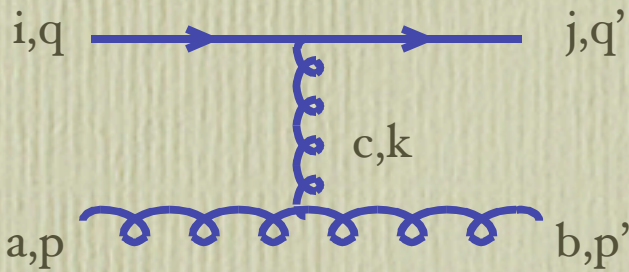
Noting that the result must be symmetric under  $s \leftrightarrow u$  exchange, and setting  $N_c=3$ , we finally obtain:

$$\overline{\square_{col,spin}} |M|^2 = \frac{4}{9} \frac{s^2 + u^2}{t^2}$$

which turns out to be the exact result!

# Quark-gluon and gluon-gluon scattering

We repeat the exercise in the more complex case of qg scattering, assuming the dominance of the t-channel gluon-exchange diagram:



$$\sim f^{abc} \square_{ij}^c 2p_\mu \frac{1}{t} 2q_\mu = 2 \frac{s}{t} f^{abc} \square_{ij}^c$$

Using the colour algebra results, and enforcing the  $s \leftrightarrow u$  symmetry, we get:

$$\overline{\square_{col,spin}} |M|^2 = \frac{s^2 + u^2}{t^2}$$

which differs by only 20% from the exact result even in the large-angle region, at  $90^\circ$

$$\overline{\square_{col,spin}} |M|^2 = \frac{s^2 + u^2}{t^2} - \frac{4s^2 + u^2}{9us}$$

In a similar way we obtain for gg scattering (using the  $t \leftrightarrow u$  symmetry):

$$\overline{\square_{col,spin}} |M(gg \rightarrow gg)|^2 = \frac{9}{2} \left( \frac{s^2}{t^2} + \frac{s^2}{u^2} \right)$$

compared to the exact result

$$\overline{\square_{col,spin}} |M(gg \rightarrow gg)|^2 = \frac{9}{2} \left( 3 - \frac{ut}{s^2} - \frac{us}{t^2} - \frac{st}{u^2} \right)$$

with a 20% difference at  $90^\circ$



Note that in the leading  $1/t$  approximation we get the following result:

$$\sigma_{gg} : \sigma_{qg} : \sigma_{qq} = \frac{9}{4} : 1 : \frac{4}{9}$$

and therefore

$$d\sigma_{jet} = \int dx_1 dx_2 \sum_{ij} f_i(x_1) f_j(x_2) d\sigma_{ij} = \int dx_1 dx_2 \sum_{ij} F(x_1) F(x_2) d\sigma_{gg}$$

where we defined the 'effective parton density'  $F(x)$ :

$$F(x) = g(x) + \frac{4}{9} \sum_i [q_i(x) + \bar{q}_i(x)]$$

As a result jet data cannot be used to extract separately gluon and quark densities. On the other hand, assuming an accurate knowledge of the quark densities (say from HERA), jet data can help in the determination of the gluon density

**Exercise:** prove that the  $1/t^2$  behaviour of the cross-section implies Rutherford's scattering law.

Event

rates in

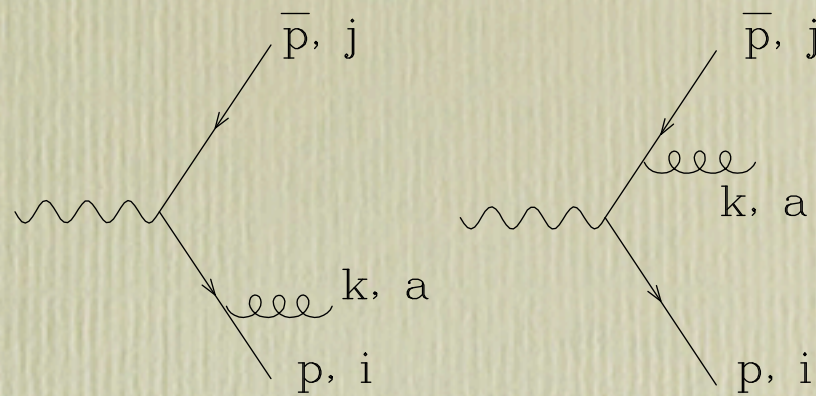
PbPb:

Channel	Barrel	Barrel+Endcap
jet+jet, $E_T^{\text{jet}} > 100$ GeV	$2.1 \times 10^6$	$4.3 \times 10^6$

# Final-state evolution

- Typical final state resulting from a jet includes many particles
- How can a calculation of a  $2 \rightarrow 2$  cross-section have anything to do with reality? What are the quantities which can be properly described by such calculation?
- Hadronization takes place at time scales much larger than the hard  $2 \rightarrow 2$  scattering ( $1/\Lambda_{\text{QCD}} \gg 1/p_{\text{T}}$ ). What happens between the hard process and hadronization can be described by perturbative QCD. However hadronization itself is a phenomenon of catastrophic intensity, which could totally disrupt the structure of the final state, by forcing any pair of colour-connected partons which are separated by more than  $1/\Lambda_{\text{QCD}}$  to bind together.
- Fortunately, QCD is kind enough to ensure that the perturbative evolution prepares a partonic state which will be left almost unperturbed by hadronization. We'll now discuss how.

# Soft gluon emission



$$\begin{aligned}
 A &= \bar{u}(p)\epsilon(k)(ig) \frac{-i}{\not{p} + \not{k}} \Gamma^\mu v(\bar{p}) \lambda_{ij}^a + \bar{u}(p) \Gamma^\mu \frac{i}{\not{p} + \not{k}} (ig)\epsilon(k) v(\bar{p}) \lambda_{ij}^a \\
 &= \left[ \frac{g}{2p \cdot k} \bar{u}(p)\epsilon(k) (\not{p} + \not{k}) \Gamma^\mu v(\bar{p}) - \frac{g}{2\bar{p} \cdot k} \bar{u}(p) \Gamma^\mu (\not{p} + \not{k}) \epsilon(k) v(\bar{p}) \right] \lambda_{ij}^a
 \end{aligned}$$

$p \cdot k = p_0 k_0 (1 - \cos\theta)$  singularities for collinear ( $\cos\theta \rightarrow 1$ ) or soft ( $k_0 \rightarrow 0$ ) emission

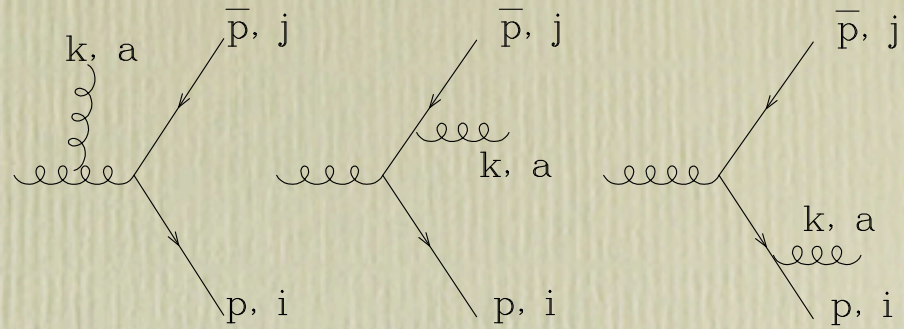
Collinear emission does not alter the global structure of the final state, since it preserves its “pencil-like-ness”. Soft emission at large angle, however, could spoil the structure, and leads to strong interferences between emissions from different legs. So soft emission needs to be studied in more detail.

In the soft ( $k_0 \rightarrow 0$ ) limit the amplitude simplifies and factorizes as follows:

$$A_{soft} = g \lambda_{ij}^a \left( \frac{p \cdot \epsilon}{p \cdot k} - \frac{\bar{p} \cdot \epsilon}{\bar{p} \cdot k} \right) A_{Born}$$

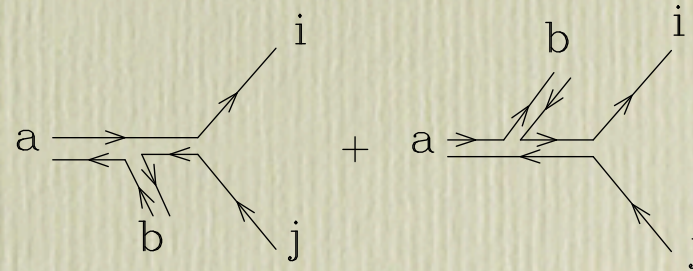
**Factorization:** it is the expression of the independence of long-wavelength (soft) emission on the nature of the hard (short-distance) process.

Similar, but more structured, result in the case of more complex colour configurations:



$$A_{soft} = g (\square^a \square^b)_{ij} \left[ \frac{Q \square}{Qk} - \frac{\bar{p} \square}{pk} \right] + g (\square^b \square^a)_{ij} \left[ \frac{p \square}{pk} - \frac{Q \square}{Qk} \right]$$

The two terms correspond to the two possible ways colour can flow in these diagrams:



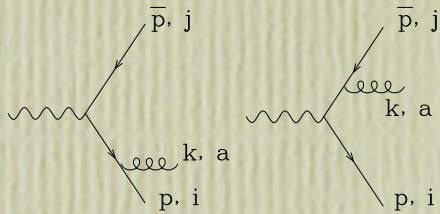
The interference between the two colour structures is suppressed by  $1/N_c^2$

$$\sum_{a,b,i,j} |(\square^a \square^b)_{ij}|^2 = \sum_{a,b} \text{tr} (\square^a \square^b \square^b \square^a) = \frac{N^2 - 1}{2} C_F = \mathcal{O}(N^3)$$

$$\sum_{a,b,i,j} (\square^a \square^b)_{ij} [(\square^b \square^a)_{ij}]^* = \sum_{a,b} \text{tr} (\square^a \square^b \square^a \square^b) = \frac{N^2 - 1}{2} \underbrace{\left( C_F - \frac{C_A}{2} \right)}_{-\frac{1}{2N}} = \mathcal{O}(N)$$

As a result, the emission of a soft gluon can be described, to the leading order in  $1/N_c^2$ , as the incoherent sum of the emission from the two colour currents

# Angular ordering in soft-gluon emission



$$d\Omega_g = \int |A_{soft}|^2 \frac{d^3k}{(2\pi)^3 2k^0} \int |A_0|^2 \frac{-2p^\mu \bar{p}^\nu}{(pk)(\bar{p}k)} g^2 \int \int \mu^* \frac{d^3k}{(2\pi)^3 2k^0}$$

$$= d\Omega_0 \frac{C_F}{\pi} \frac{dk^0}{k^0} \frac{d\Omega}{2\pi} \frac{1 - \cos\theta_{ij}}{(1 - \cos\theta_{ik})(1 - \cos\theta_{jk})} d\cos\theta$$

You can easily prove that:

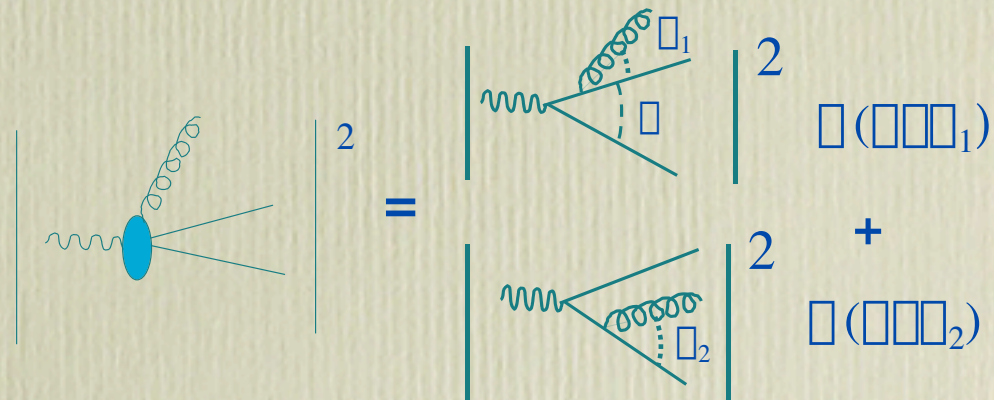
$$\frac{1 - \cos\theta_{ij}}{(1 - \cos\theta_{ik})(1 - \cos\theta_{jk})} = \frac{1}{2} \left[ \frac{\cos\theta_{jk} - \cos\theta_{ij}}{(1 - \cos\theta_{ik})(1 - \cos\theta_{jk})} + \frac{1}{1 - \cos\theta_{ik}} \right] + \frac{1}{2} [i \leftrightarrow j] \equiv W_{(i)} + W_{(j)}$$

where:  $W_{(i)} \rightarrow$  finite if  $k \parallel j$  ( $\cos\theta_{jk} \rightarrow 1$ )  
 $W_{(j)} \rightarrow$  finite if  $k \parallel i$  ( $\cos\theta_{ik} \rightarrow 1$ )

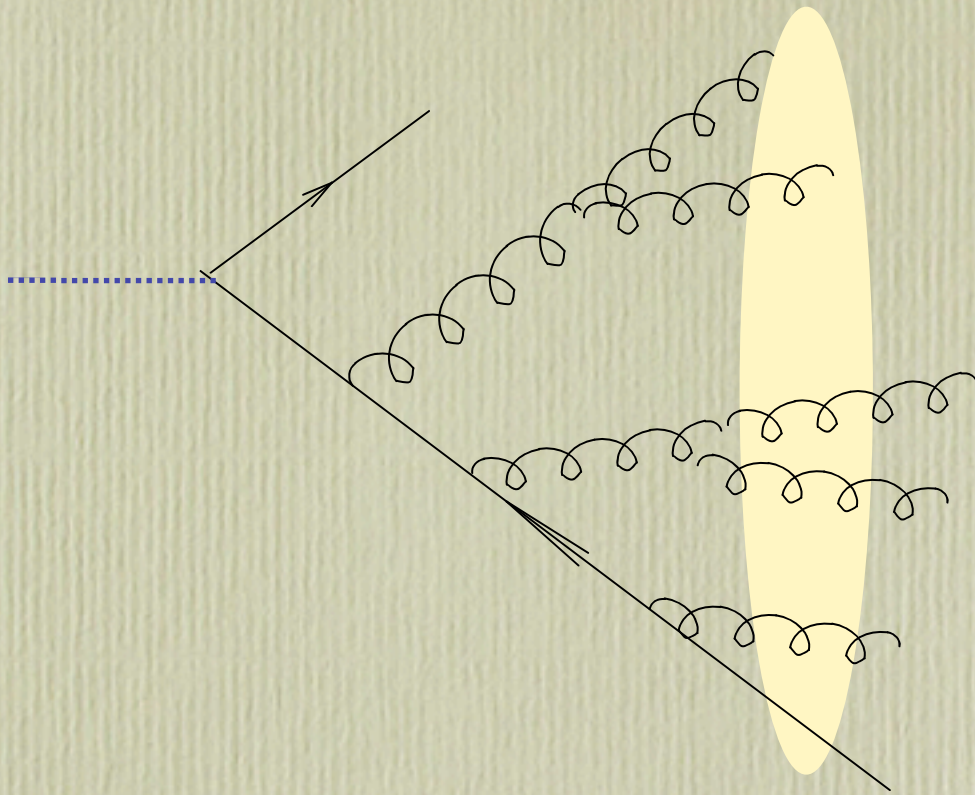
The probabilistic interpretation of  $W_{(i)}$  and  $W_{(j)}$  is a priori spoiled by their non-positivity. However, you can prove that after azimuthal averaging:

$$\int \frac{d\Omega}{2\pi} W_{(i)} = \frac{1}{1 - \cos\theta_{ik}} \text{ if } \theta_{ik} < \theta_{ij}, \quad 0 \text{ otherwise}$$

$$\int \frac{d\Omega}{2\pi} W_{(j)} = \frac{1}{1 - \cos\theta_{jk}} \text{ if } \theta_{jk} < \theta_{ij}, \quad 0 \text{ otherwise}$$

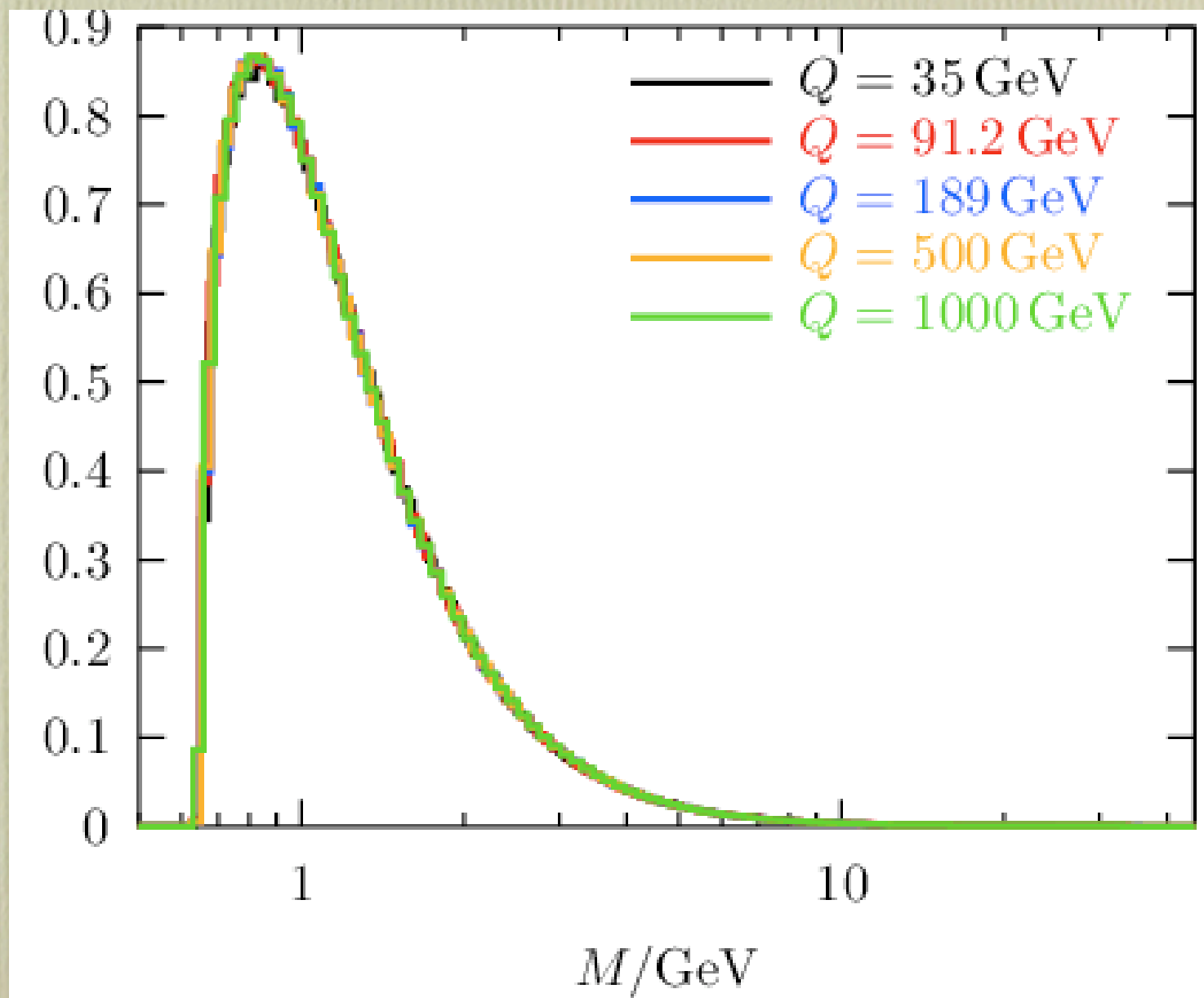


Further branchings will obey angular ordering relative to the new angles. As a result emission angles get smaller and smaller, squeezing the jet



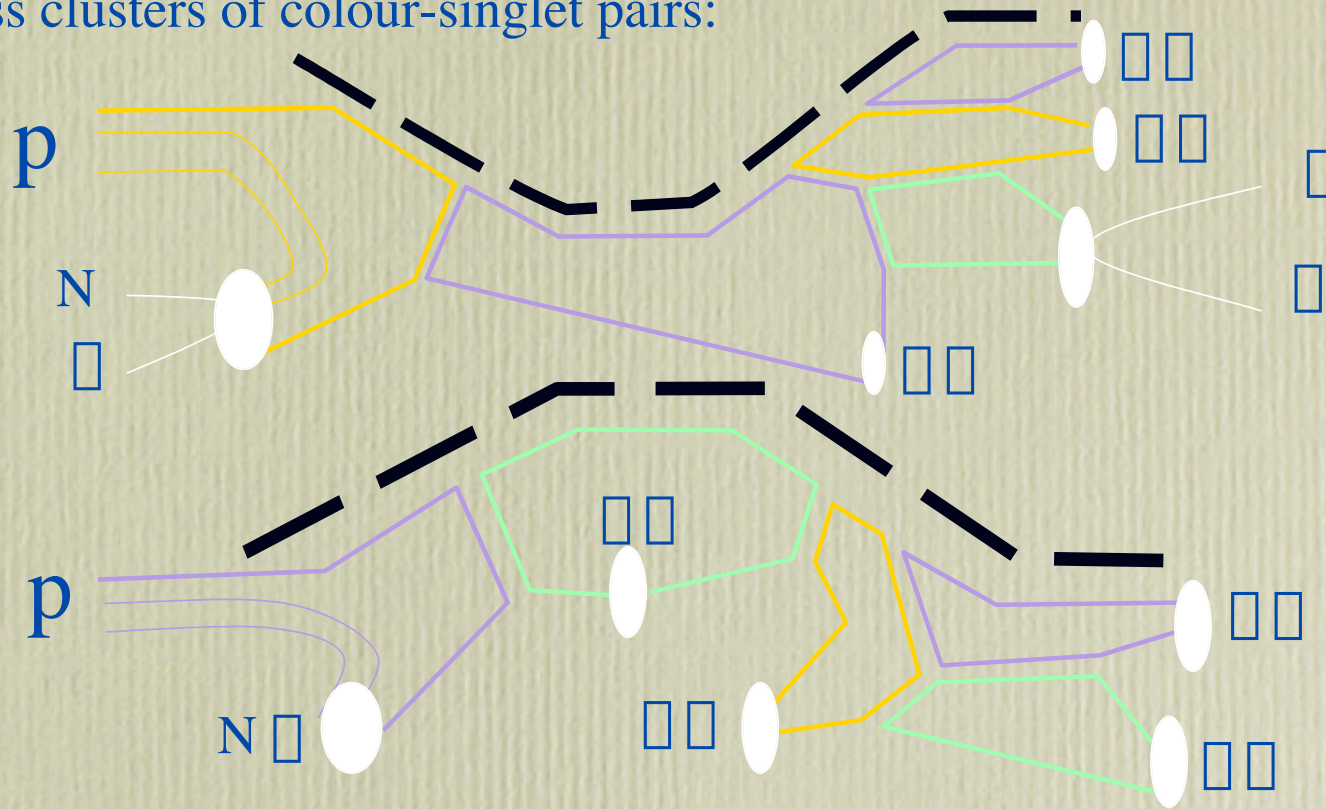
Total colour charge of the system is equal to the quark colour charge. Treating the system as the incoherent superposition of  $N$  gluons would lead to artificial growth of gluon multiplicity. Angular ordering enforces coherence, and leads to the proper evolution with energy of particle multiplicities.

The structure of the perturbative evolution therefore leads naturally to the clustering in phase-space of colour-singlet parton pairs (“preconfinement”). Long-range correlations are strongly suppressed. Hadronization will only act locally, on low-mass colour-singlet clusters.



# Hadronization

At the end of the perturbative evolution, the final state consists of quarks and gluons, forming, as a result of angular-ordering, low-mass clusters of colour-singlet pairs:



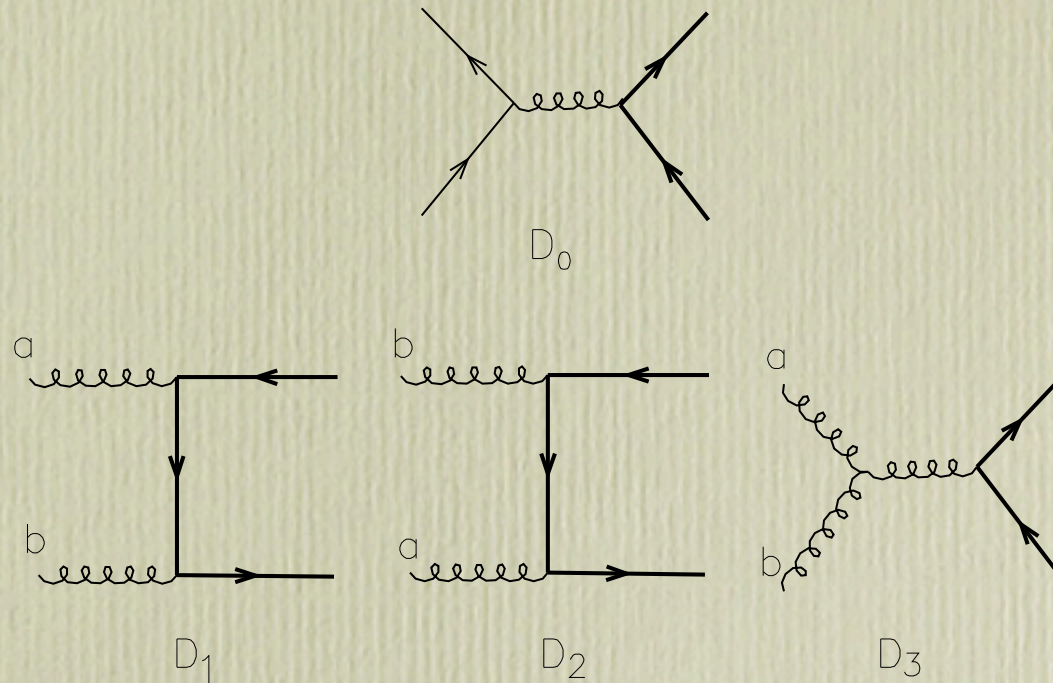
Thanks to the cluster pre-confinement, hadronization is local and independent of the nature of the primary hard process, as well as of the details of how hadronization acts on different clusters. Among other things, one therefore expects:

$$\mathbf{N(\text{pions}) = C N(\text{gluons}),}$$
$$\mathbf{C = \text{constant} \sim 2}$$



# Heavy quark production

(for pedagogical introduction, see: hep-ph/9711337)



Singularity structure of t-channel propagator:

$$(p_1 - Q)^2 - m^2 = -2p_1 \cdot Q = -\frac{\hat{s}}{2}(1 - \cos\theta)$$

$$2p_1 \cdot Q \geq \frac{\hat{s}}{2}(1 - \cos\theta) = \frac{\hat{s}}{2(1 + \cos\theta)}(1 - \cos^2\theta) = \frac{2m^2}{1 + \cos\theta} \geq m^2$$

$\Rightarrow$  Total HQ cross-sections are finite, and calculable in pQCD

Matrix elements:

$$\frac{1}{g^4} \overline{\Sigma} |M(q\bar{q} \rightarrow Q\bar{Q})|^2 = \frac{V}{2N^2} (\tau_1^2 + \tau_2^2 + \frac{\rho}{2})$$

$$\frac{1}{g^4} \overline{\Sigma} |M(gg \rightarrow Q\bar{Q})|^2 = \frac{1}{2VN} \left( \frac{V}{\tau_1\tau_2} - 2N^2 \right) \left( \tau_1^2 + \tau_2^2 + \rho - \frac{\rho^2}{4\tau_1\tau_2} \right)$$

$$\tau_{1,2} = 2 \frac{p_{1,2} \cdot Q}{\hat{s}} = \frac{1 \mp \beta \cos \Theta}{2}, \quad \rho = \frac{4m^2}{\hat{s}}, \quad \hat{s} = (p_1 + p_2)^2$$

Phase-space:

$$d\phi_{(2)} \equiv \frac{1}{2\hat{s}} \frac{d^2Q}{(2\pi)^3 2Q^0} \frac{d^3\bar{Q}}{(2\pi)^3 2\bar{Q}^0} (2\pi)^4 \delta^4(P_{in} - P_{out}) = \frac{\pi}{2\hat{s}} \left( \frac{1}{4\pi} \right)^2 \beta d(\cos \theta)$$

Total cross-section:

$$\hat{\sigma}(q\bar{q} \rightarrow Q\bar{Q}) = \frac{\alpha_s^2}{m^2} \left( \frac{V}{N^2} \right) \frac{\pi\beta}{24} \rho(2 + \rho) \xrightarrow{\hat{s} \rightarrow \infty} \frac{1}{\hat{s}}$$

$$\hat{\sigma}(gg \rightarrow Q\bar{Q}) = \frac{\alpha_s^2}{m^2} \left( \frac{1}{NV} \right) \frac{\pi\beta}{24} \rho \left[ 3\mathcal{L}(\beta) (\rho^2 + 2V(\rho + 1)) \right. \\ \left. + 2(V - 2)(1 + \rho) + \rho(6\rho - N^2) \right] \xrightarrow{\hat{s} \rightarrow \infty} \frac{1}{\hat{s}} \mathcal{L}(\beta)$$

$$\mathcal{L}(\beta) = \frac{1}{\beta} \log \left( \frac{1 + \beta}{1 - \beta} \right) - 2$$

Differential distributions:

$$\frac{d\sigma}{dy d\bar{y} dp_T^2} = \frac{\pi}{4m_T^4} \frac{1}{[1 + \cosh(y - \bar{y})]^2} \frac{1}{(4\pi^2)} \times \sum_{ij} x_1 f_i(x_1) x_2 f_j(x_2) \overline{\Sigma} |M(ij \rightarrow Q\bar{Q})|^2$$

Very strong rapidity correlation:  $\Delta y < 1$

# Total cross-sections

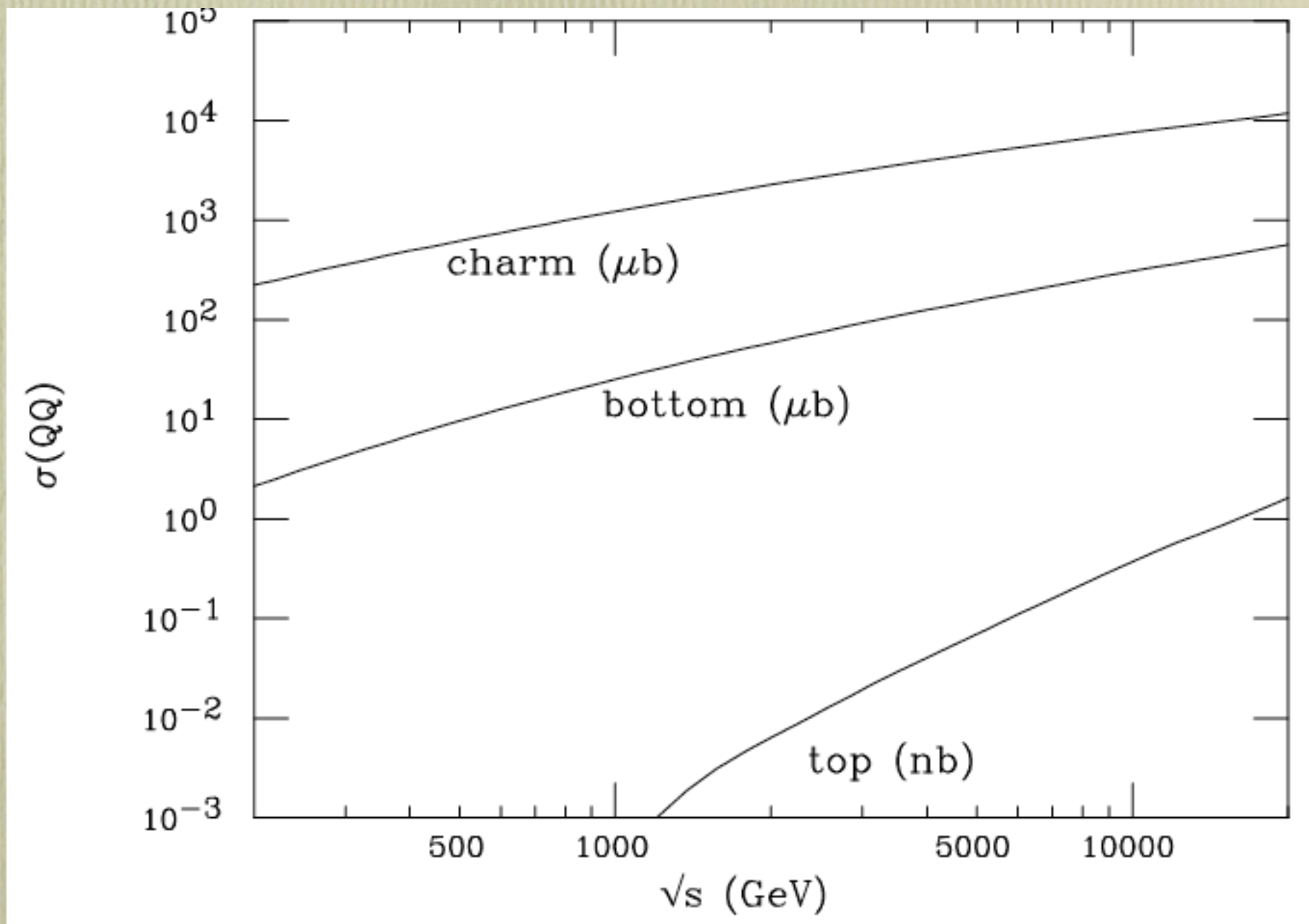
Table 1: Production cross sections for charm pairs in  $pp$  collisions at 14 TeV and 5.5 TeV. The penultimate column gives the ratios of cross sections at the two energies for the various parameter sets. The last column gives the ratios, normalized to the ratio obtained with  $\mathcal{P} = \text{I}$ .

I-VI: different input parameters

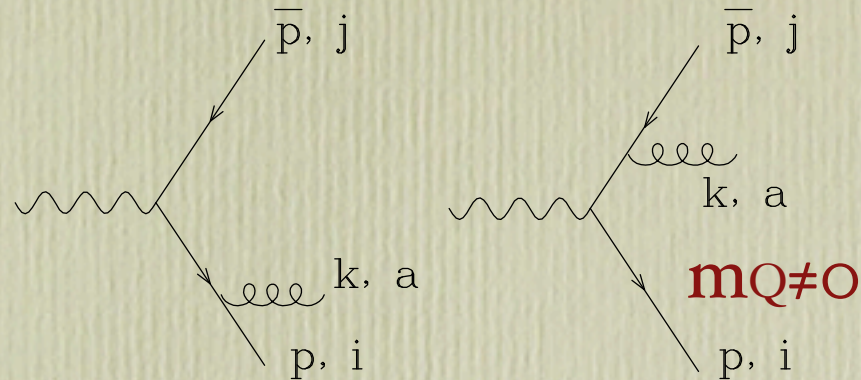
$\mathcal{P}$	$\sigma_{14}$ (mb)	$K = \sigma_{\text{NLO}}/\sigma_{\text{LO}}$	$\sigma_{5.5}$ (mb)	$R(\mathcal{P}) = \sigma_{5.5}/\sigma_{14}$	$R(\mathcal{P})/R(\mathcal{P} = \text{I})$
I	10.4	1.7	5.4	0.52	1
II	16.7	1.7	9.2	0.55	1.06
III	6.8	1.7	3.4	0.50	0.96
IV	7.3	2.1	3.7	0.51	0.98
V	8.57	1.8	4.2	0.49	0.94
VI	10.6	1.8	5.3	0.50	0.96

Table 2: Production cross sections for bottom pairs in  $pp$  collisions at 14 TeV and 5.5 TeV. The penultimate column gives the ratios of cross sections at the two energies for the various parameter sets. The last column gives the ratios, normalized to the ratio obtained with  $\mathcal{P} = \text{I}$ .

$\mathcal{P}$	$\sigma_{14}$ (mb)	$K = \sigma_{\text{NLO}}/\sigma_{\text{LO}}$	$\sigma_{5.5}$ (mb)	$R(\mathcal{P}) = \sigma_{5.5}/\sigma_{14}$	$R(\mathcal{P})/R(\mathcal{P} = \text{I})$
I	0.43	2.3	0.17	0.40	1
II	0.51	2.4	0.20	0.39	0.98
III	0.37	2.3	0.15	0.41	1.03
IV	0.66	1.4	0.26	0.39	0.98
V	0.20	3.2	0.088	0.44	1.1
VI	0.40	2.4	0.17	0.43	1.08
VII	0.45	2.4	0.18	0.40	1



# Evolution of a heavy quark

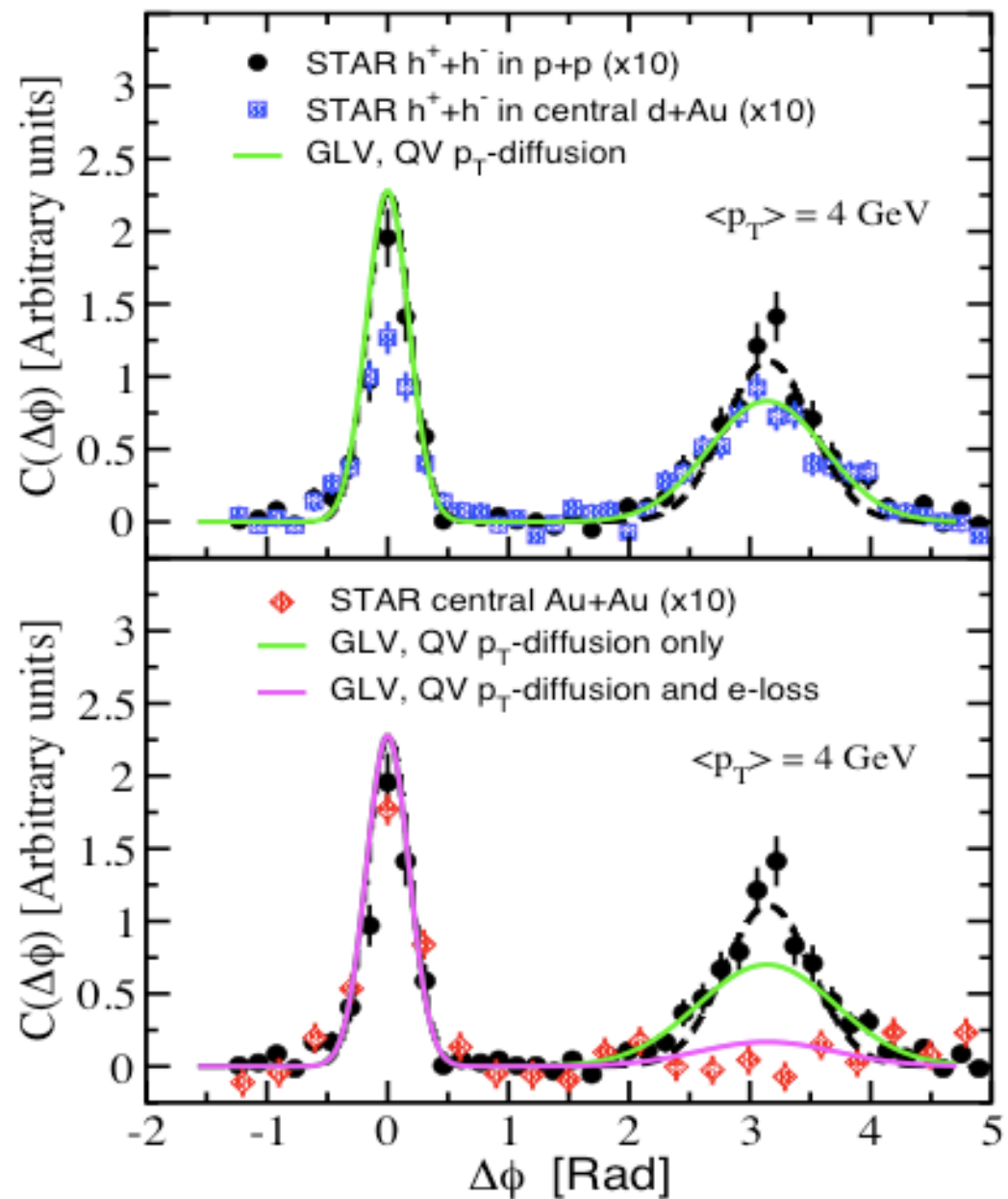
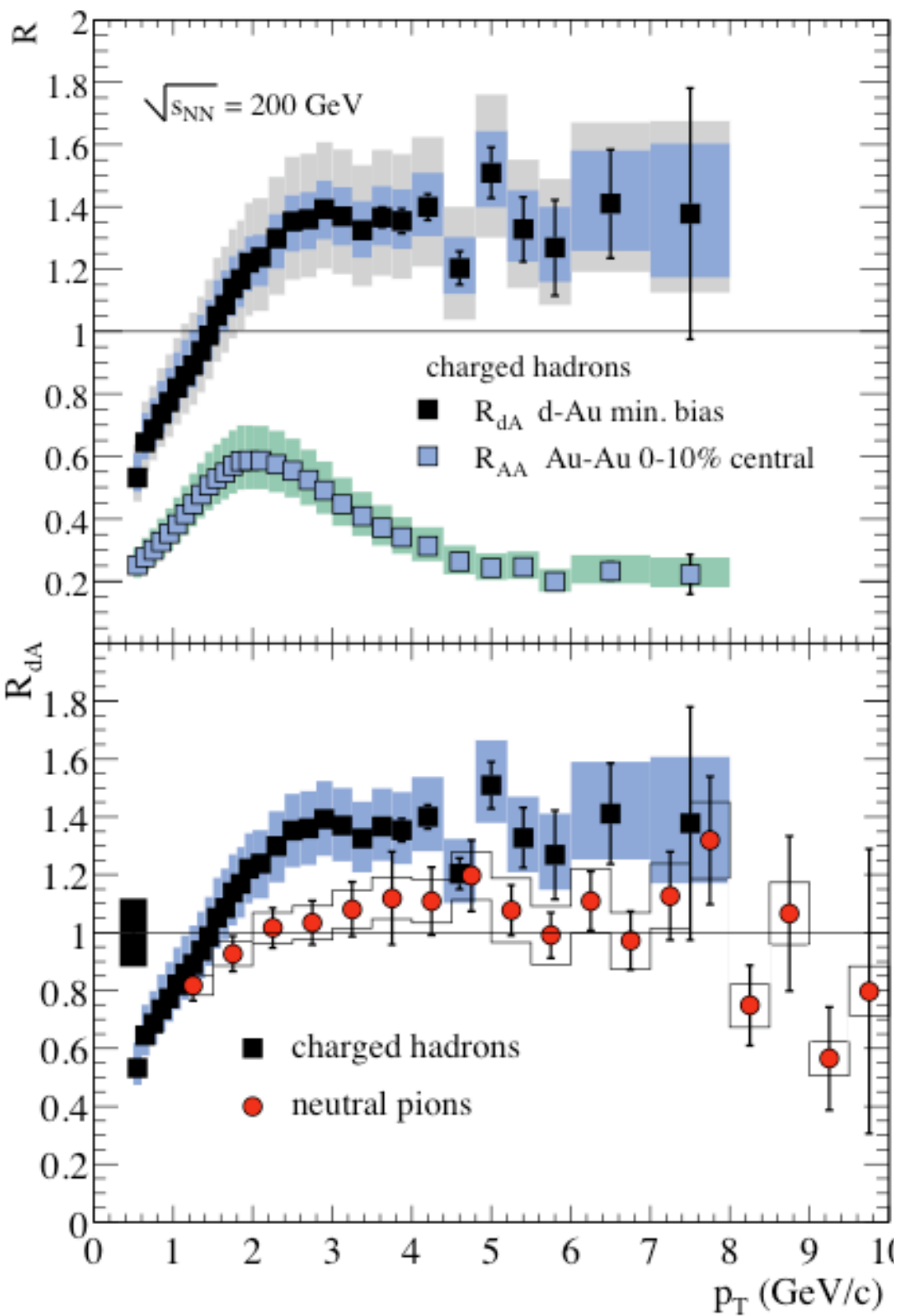


$$A_{soft} = g_{ij}^a \left( \frac{p \cdot \epsilon}{p \cdot k} - \frac{\bar{p} \cdot \epsilon}{\bar{p} \cdot k} \right) A_{Born} \text{ same as for } m_Q=0. \text{ However now:}$$

$$pk = p_0 k_0 (1 - \beta \cos \theta),$$

where  $\beta$  is the quark velocity,  $\beta < 1$ .

Therefore radiation in the very forward region (collinear radiation) is suppressed. A massive quark therefore loses less energy during the evolution, and its “quenching profile” will be different than the one of a light quark or gluon.



# Some interesting questions

\* Plot  $dN/d\varphi$  vs  $d/D$ . Possible?

\* Particle  $p_T$  in  $J_2$  is degraded; this means that more particles must share the same amount of momentum  $\rightarrow$  increased multiplicity. Can it be measured?

\* What do we learn about the QGP from the study of quenching? What is the quantitative relation between the parameters of the **QGP Eq of State** and the fragmentation properties of  $J_2$ ?

\* **What are the PDG-like parameters that we can extract from these measurements?**

